

REPORT

CLINICAL TRIALS

Fecal microbiota transplant promotes response in immunotherapy-refractory melanoma patients

Erez N. Baruch^{1,2,*†}, Ilan Youngster^{3,4}, Guy Ben-Betzalel¹, Rona Ortenberg¹, Adi Lahat⁵, Lior Katz⁶, Katerina Adler⁷, Daniela Dick-Necula⁸, Stephen Raskin^{4,9}, Naamah Bloch¹⁰, Daniil Rotin⁸, Liat Anafi⁸, Camila Avivi⁸, Jenny Melnichenko¹, Yael Steinberg-Silman¹, Ronac Mamtani¹¹, Hagit Harati¹, Nethanel Asher¹, Ronnie Shapira-Frommer¹, Tal Brosh-Nissimov¹², Yael Eshet^{4,8,13}, Shira Ben-Simon¹⁰, Oren Ziv¹⁰, Md Abdul Wadud Khan¹⁴, Moran Amit¹⁵, Nadim J. Ajami¹⁴, Iris Barshack^{4,8}, Jacob Schachter^{1,4}, Jennifer A. Wargo^{14,16}, Omry Koren¹⁰, Gal Markel^{1,2,17,*†}, Ben Boursi^{4,18,19,†}

The gut microbiome has been shown to influence the response of tumors to anti-PD-1 (programmed cell death-1) immunotherapy in preclinical mouse models and observational patient cohorts. However, modulation of gut microbiota in cancer patients has not been investigated in clinical trials. In this study, we performed a phase 1 clinical trial to assess the safety and feasibility of fecal microbiota transplantation (FMT) and reinduction of anti-PD-1 immunotherapy in 10 patients with anti-PD-1-refractory metastatic melanoma. We observed clinical responses in three patients, including two partial responses and one complete response. Notably, treatment with FMT was associated with favorable changes in immune cell infiltrates and gene expression profiles in both the gut lamina propria and the tumor microenvironment. These early findings have implications for modulating the gut microbiota in cancer treatment.

Immunotherapy to inhibit the programmed cell death-1 (PD-1) checkpoint protein in metastatic melanoma patients has demonstrated durable complete response (CR) rates of 10 to 20% (1). However, most of the patients do not respond to PD-1 blockade, and many of the partially responding patients eventually progress (1). Extensive research efforts have been undertaken to overcome the resistance to anti-PD-1 therapy. One of the most promising leads involves modulation of the gut microbiota (2–4), which has been shown to have a profound effect on the development and function of the immune system (5). Although no specific bacterial taxa have been consistently associated with clinical response to immunotherapy (6), fecal microbiota transplantation (FMT)—which transfers the entire gut microbiota from one host to another—has demonstrated promising results in preclinical models (2–4). Compared with mice that received FMT from melanoma patients not responding to anti-PD-1 therapy, mice that received FMT from responders demonstrated increased intratumoral CD8⁺ T cell

infiltration and enhanced overall effectiveness of anti-PD-1 therapy (2, 3). On the basis of these data, we designed a phase 1 clinical trial (NCT03353402) to assess the safety, feasibility, and immune cell impact of FMT and reinduction of anti-PD-1 immunotherapy in patients with refractory metastatic melanoma.

The trial included two FMT donors who had previously been treated with anti-PD-1 monotherapy for metastatic melanoma and had achieved a CR for at least 1 year (table S1 and materials and methods). Patients were considered eligible FMT recipients if they had a diagnosis of metastatic melanoma and had progressed on at least one line of anti-PD-1 therapy. Recipients harboring a BRAF-V600E mutation must have also progressed on BRAF-targeted therapy. As part of the trial's protocol, recipients underwent an initial native microbiota depletion phase in which they were administered with orally ingested antibiotics (vancomycin and neomycin) for 72 hours (Fig. 1A). FMT was then performed by means of both a colonoscopy (protocol day 0) and the administration of oral stool capsules fol-

lowed by reinduction of anti-PD-1 therapy (nivolumab). Six combined treatment cycles composed of anti-PD-1 infusions (nivolumab at standard dose) and additional stool capsules (maintenance FMT) were administered every 14 days until day 90. Each recipient underwent positron emission tomography combined with computed tomography (PET-CT) imaging before the trial and on day 65. Response to treatment was defined as an objective tumor regression per imaging according to iRECIST criteria (response evaluation criteria in solid tumors, modified for immunotherapy) (7). Objective responders and recipients who demonstrated a clinical benefit to the treatment continued anti-PD-1 beyond day 90 as monotherapy and underwent consecutive PET-CTs in intervals of 6 to 8 weeks until disease progression.

Correlative studies included stool, gut, and tumor analyses (see materials and methods). 16S ribosomal RNA (rRNA) gene and metagenomics sequencing were conducted on stool samples that were collected from recipients up to 1 week before the native microbiota depletion phase (defined as pretreatment) and on stool samples collected on days 7, 31, and 65. Donor stool samples were collected during the fecal donation period. Gut and tumor biopsies were collected pretreatment and at days 31 and 70, respectively. Infiltration and activity of immune cells in the tissue samples were assessed using immunohistochemical (IHC) and bulk RNA sequencing (RNA-seq). In cases where no specific gene differed in a statistically significant manner, gene set testing was conducted using the Gene Ontology (GO) dataset. Recipient 2 refused to undergo post-treatment biopsies and withdrew consent immediately after the day-65 imaging assessment, leaving nine available recipients for gut and tumor tissue assessment.

Ten recipients with confirmed progression on anti-PD-1 therapy were enrolled and treated between June 2018 and March 2019 (Table 1 and table S2). Recipients were assigned to receive FMT from one of the two available donors, alternating between donor 1 and donor 2. The median recipient age was 66 years [interquartile range (IQR), 49 to 68 years], the majority were males (70%), and the median elapsed time from the last previous dose of anti-PD-1 to the first dose of the current trial was 113 days

¹The Ella Lemelbaum Institute for Immuno-Oncology, Sheba Medical Center, Tel-HaShomer, Israel. ²Department of Clinical Immunology and Microbiology, Sackler Faculty of Medicine, Tel Aviv University, Tel Aviv, Israel. ³Pediatric Division and the Microbiome Research Center, Shamir (Assaf Harofeh) Medical Center, Be'er Ya'akov, Israel. ⁴School of Medicine, Sackler Faculty of Medicine, Tel Aviv University, Tel Aviv, Israel. ⁵Department of Gastroenterology, Sheba Medical Center, Tel HaShomer, Israel. ⁶Department of Gastroenterology, Hadassah Medical Center, Jerusalem, Israel. ⁷Department of Mathematics, Bar Ilan University, Ramat Gan, Israel. ⁸Institute of Pathology, Sheba Medical Center, Tel-HaShomer, Israel. ⁹Radiological Institute, Sheba Medical Center, Tel HaShomer, Israel. ¹⁰Azieli Faculty of Medicine, Bar Ilan University, Safed, Israel. ¹¹Division of Hematology and Oncology, University of Pennsylvania, Philadelphia, PA, USA. ¹²Infectious Diseases Unit, Assuta Ashdod University Hospital, Ashdod, Israel. ¹³Department of Nuclear Medicine, Sheba Medical Center, Tel HaShomer, Israel. ¹⁴Program for Innovative Microbiome and Translational Research, Department of Genomic Medicine, The University of Texas MD Anderson Cancer Center, Houston, TX, USA. ¹⁵Department of Head and Neck Surgery, The University of Texas MD Anderson Cancer Center, Houston, TX, USA. ¹⁶Department of Surgical Oncology, The University of Texas MD Anderson Cancer Center, Houston, TX, USA. ¹⁷Talpiot Medical Leadership Program, Sheba Medical Center, Tel HaShomer, Israel. ¹⁸Center for Clinical Epidemiology and Biostatistics, University of Pennsylvania, Philadelphia, PA, USA. ¹⁹Department of Oncology, Sheba Medical Center, Tel HaShomer, Israel.

*Corresponding author. Email: erezbaruch@mail.tau.ac.il (E.N.B.); gal.markel@sheba.health.gov.il (G.M.) †Present addresses: Program for Innovative Microbiome and Translational Research, Department of Genomic Medicine, The University of Texas MD Anderson Cancer Center, Houston, TX, USA, and Department of Internal Medicine, McGovern Medical School at The University of Texas Health Science Center, Houston, TX, USA. ‡These authors contributed equally to this work.

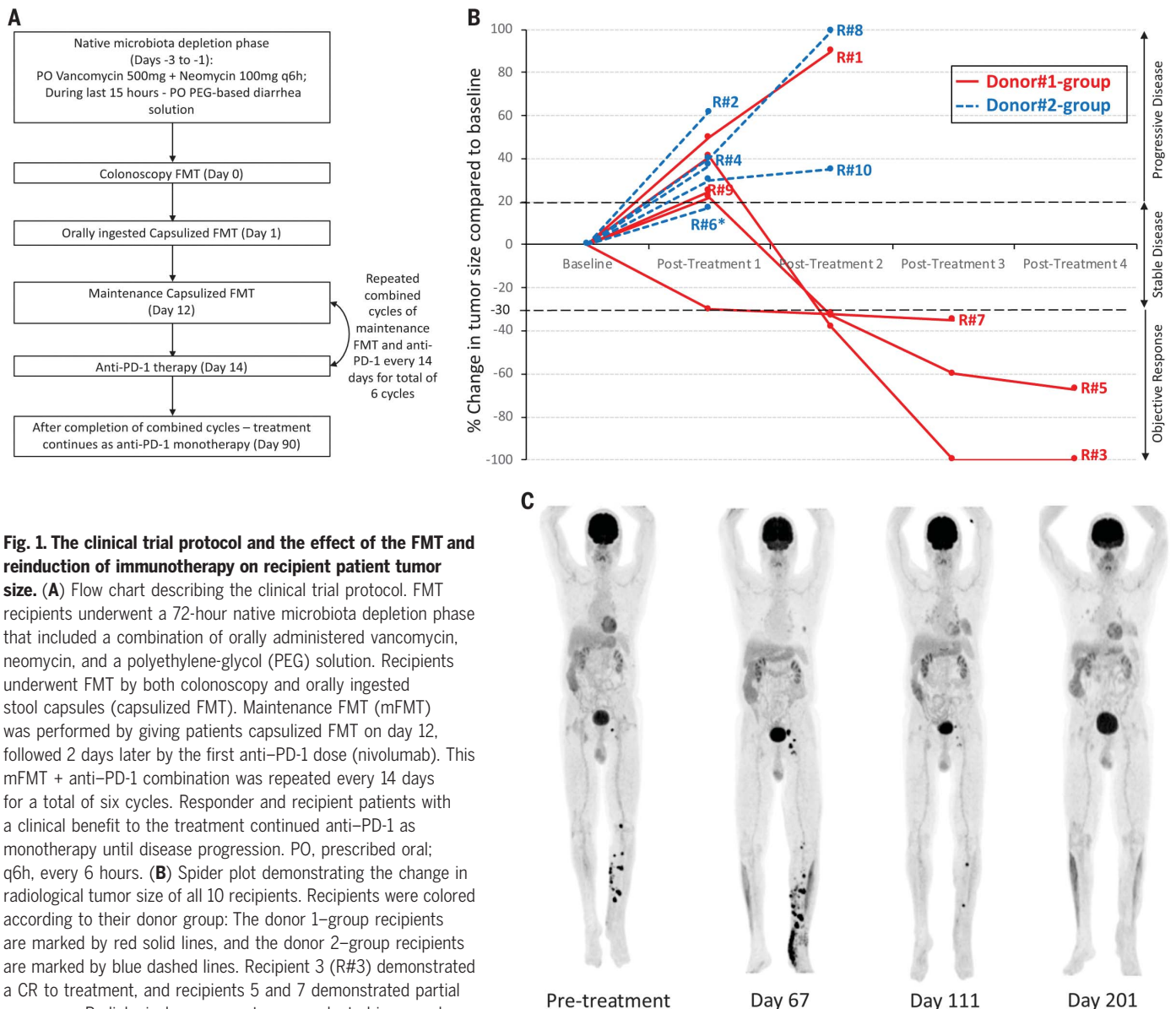


Fig. 1. The clinical trial protocol and the effect of the FMT and reinduction of immunotherapy on recipient patient tumor size. (A) Flow chart describing the clinical trial protocol. FMT recipients underwent a 72-hour native microbiota depletion phase that included a combination of orally administered vancomycin, neomycin, and a polyethylene-glycol (PEG) solution. Recipients underwent FMT by both colonoscopy and orally ingested stool capsules (capsulized FMT). Maintenance FMT (mFMT) was performed by giving patients capsulized FMT on day 12, followed 2 days later by the first anti-PD-1 dose (nivolumab). This mFMT + anti-PD-1 combination was repeated every 14 days for a total of six cycles. Responder and recipient patients with a clinical benefit to the treatment continued anti-PD-1 as monotherapy until disease progression. PO, prescribed oral; q6h, every 6 hours. (B) Spider plot demonstrating the change in radiological tumor size of all 10 recipients. Recipients were colored according to their donor group: The donor 1-group recipients are marked by red solid lines, and the donor 2-group recipients are marked by blue dashed lines. Recipient 3 (R#3) demonstrated a CR to treatment, and recipients 5 and 7 demonstrated partial responses. Radiological assessment was conducted in accordance with the immune response evaluation criteria in solid tumors (RECIST) (7) and included measurements of target and new target lesions. The asterisk indicates that recipient 6 was excluded from the trial after the first posttreatment imaging study because of unstable metastatic brain disease (hemorrhage into a brain metastasis that was known before inclusion in the trial). (C) Recipient 3 PET-CT imaging. The metastatic lesions, represented as black emission areas, were concentrated in the left leg and groin (inguinal). As a result of the treatment, the metastases had initially increased in size and new lesions appeared (day 67). However, a complete resolution of all lesions was demonstrated in consecutive follow-up imaging studies. The initial tumor size increment was likely caused by the substantial increase in CD8⁺ T cell intratumoral infiltration that was observed in this patient (14 cells/mm² pretreatment versus 736 cells/mm² on day 70; see below, Fig. 3, E to G), a phenomenon known as pseudoprogression (8).

(IQR, 59 to 183 days). The most common PD-L1 expression category in pretreatment tumor biopsies was $\geq 5\%$. This expression category was noted in four recipients, whereas three recipients had no pretreatment PD-L1 expression (table S2). In terms of safety results, the only observed FMT-related adverse event (AE) was mild bloating between days 3 and 15 in one recipient. Several mild (grade 1) immune-related adverse events (irAEs) were observed, mainly arthralgia (table S3). No moderate-to-

severe irAEs (grades 2 to 4) were observed, although five recipients had developed such irAEs during their previous anti-PD-1 treatment lines (table S4). Objective responses to treatment were demonstrated by three recipients, all of them from the donor 1 group: Recipient 3 achieved a CR, and recipients 5 and 7 achieved partial responses (Fig. 1B, Table 1, and table S5). All responders crossed the progression-free survival milestone of 6 months. Both recipients 3

and 5 demonstrated an initial increase in their metastases size followed by regression (Fig. 1, B and C, and fig. S1). This phenomenon is known as pseudoprogression (8) because the increment in metastasis radiological volumes is not caused by tumor proliferation but rather by an influx of antitumoral immune cells into the tumor. Recipient 1 (donor 1 group) demonstrated an initial mixed response with regression of some of lesions, but, overall, the disease had progressed (fig. S2).

and 5 demonstrated an initial increase in their metastases size followed by regression (Fig. 1, B and C, and fig. S1). This phenomenon is known as pseudoprogression (8) because the increment in metastasis radiological volumes is not caused by tumor proliferation but rather by an influx of antitumoral immune cells into the tumor. Recipient 1 (donor 1 group) demonstrated an initial mixed response with regression of some of lesions, but, overall, the disease had progressed (fig. S2).

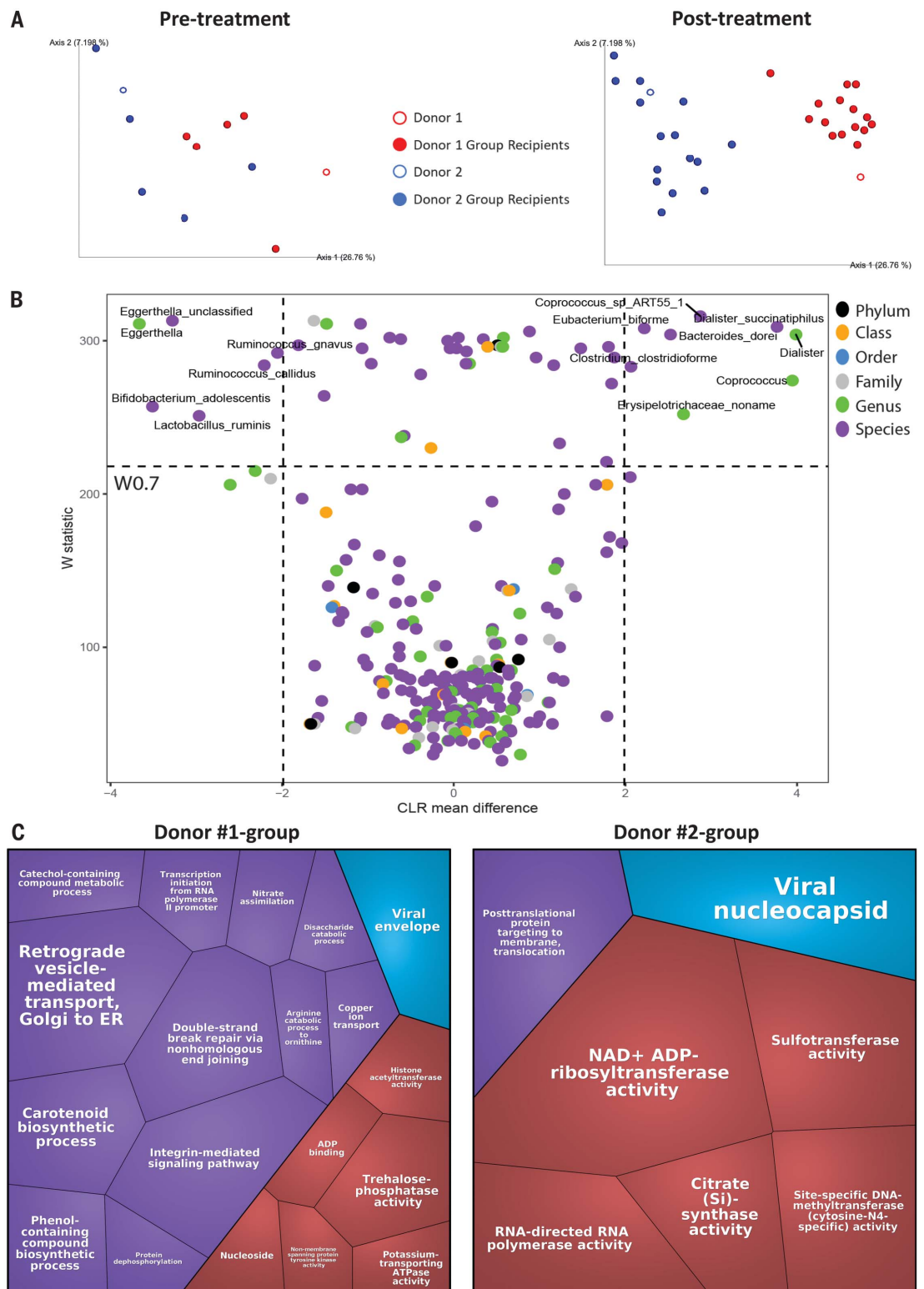
and 5 demonstrated an initial increase in their metastases size followed by regression (Fig. 1, B and C, and fig. S1). This phenomenon is known as pseudoprogression (8) because the increment in metastasis radiological volumes is not caused by tumor proliferation but rather by an influx of antitumoral immune cells into the tumor. Recipient 1 (donor 1 group) demonstrated an initial mixed response with regression of some of lesions, but, overall, the disease had progressed (fig. S2).

Fig. 2. The effect of FMT on gut microbiota composition in metastatic melanoma recipient patients.

(A) Principal components analysis (PCA) plots of patient gut microbiota compositions based on stool 16S rRNA gene sequencing dissimilarity test (β -diversity, unweighted UniFrac). The distance between samples on the plot represents their dissimilarity—the greater the distance between two samples, the higher the dissimilarity of their composition. Recipient patients were grouped according to their donors: Those who received FMT implants from donor 1 are colored in red, and those who received implants from donor 2 are colored in blue. The plots demonstrate no difference between the pretreatment recipient compositions of the two donor groups (FDR = 0.45), in contrast to a clear post-treatment donor-based division (FDR = 0.003).

(B) A volcano plot based on the ANCOM test. The plot compares the relative abundance of specific taxa between the donor 1 group (negative x axis) and the donor 2 group (positive x axis). Each donor group was composed of posttreatment samples of the relevant recipients and the donor sample. Taxa that differed between the groups with FDR $q \leq 0.05$ are presented above the horizontal dashed line. The center log transformation (CLR) mean difference on the x axis is an ANCOM calculation that is used to determine compositional differences in microbial communities. For convenience, only taxa with a mean difference above an absolute value of 2 are labeled with text. The full list of taxa that significantly differed between the two donor groups is detailed in table S7.

(C) Voronoi treemap plots of microbiota GO gene sets that were enriched among the different donor groups' microbiotas. The abundance of gene sets was compared across donors and posttreatment recipient samples. Gene sets that showed statistically significant differences between the donor 1 group and the donor 2 group and had a \log_2 differential abundance >1 (table S8) are plotted. The polygon size represents the scale of the \log_2 abundance difference—a bigger polygon represents a more abundant pathway. The GO gene sets are also colored according to their GO category: purple for biological processes, light blue for cellular components, and red for molecular functions. ER, endoplasmic reticulum; ADP, adenosine 5'-diphosphate; ATPase, adenosine triphosphatase; NAD⁺, oxidized nicotinamide adenine dinucleotide.



Stool 16S rRNA gene sequencing analysis demonstrated that posttreatment gut microbiota composition of all recipients significantly differed from their baseline [β -diversity, unweighted UniFrac, $P = 0.02$; false discovery rate (FDR) = 0.05; Fig. 2A and figs. S3 and S4]. There was no statistically significant difference between the pretreatment microbiota composition of recipients from the donor 1 group and those of the donor 2 group ($P = 0.36$; FDR = 0.45). However, posttreatment microbiota compositions of the donor 1–group recipients differed from those of the donor 2 group ($P = 0.001$; FDR = 0.003; Fig. 2A). Donor 2 had a higher microbiota richness (α -diversity, Faith's phylogenetic diversity) compared with donor 1. Accordingly, despite similar richness in the pre-

treatment compositions ($P = 0.60$; FDR = 0.77), posttreatment compositions of the donor 2 group demonstrated higher richness than those of the donor 1 group ($P < 0.001$; FDR = 0.001; fig. S5). Metagenomic sequencing was used to identify specific taxa and functional pathways that differed between the trial's groups. Overall comparison between recipient pre- and posttreatment microbiota compositions [analysis of composition of microbiomes (ANCOM) test] showed that posttreatment compositions had a higher relative abundance of the immunotherapy-favorable *Veillonellaceae* family (3) and a lower relative abundance of *Bifidobacterium bifidum*, which was reported to promote immune tolerance via regulatory T cells (9) (figs. S6 and S7). Both donors had

previously reported immunotherapy-favorable features (fig. S8 and table S6) such as high relative abundances of *Lachnospiraceae* (both donors), *Veillonellaceae* (donor 1), and *Ruminococcaceae* (donor 2) (fig. S8) (2–4). Comparison of posttreatment recipient microbiota compositions by their assigned donors demonstrated that the donor 1 group was characterized by a higher relative abundance of taxa like *Bifidobacterium adolescentis* (Fig. 2B), whereas the donor 2 group had a high relative abundance of taxa like *Ruminococcus bromii* (table S7)—both of which have been previously described as immunotherapy favorable (2, 3). The pretreatment microbiota compositions of the three responding patients (recipients 3, 5, and 7) did not differ from the pretreatment

Table 1. Clinical characteristics of patients receiving FMT and reinduction of anti-PD-1 treatment. The time from previous anti-PD-1 treatment dose to the first trial dose was calculated from the most recent anti-PD-1 treatment dose to the day of the first anti-PD-1 treatment in the clinical trial. The percentage of viable tumor was calculated as the percentage of viable tumor out of the entire tumor tissue which was examined in a hematoxylin and eosin (H&E) slide of the tumor biopsy (see materials and methods). Clinical responses were based on the iRECIST (7). Response category "None" represents iRECIST-confirmed progressive disease. Recipient 2 did not consent to undergo repeated tumor and gut biopsies, and hence, the percentage of viable tumor is presented as not available (N/A). Additional clinical data per donor and recipient can be found in the supplementary materials (tables S1 and S2, respectively). D, dabrafenib; T, trametinib; Nivo, nivolumab; Pembro, pembrolizumab; Ipi, ipilimumab; T-VEC, talimogene laherparepvec; TIL, adoptive cell therapy composed of tumor-infiltrating lymphocytes.

FMT donor group	Recipient	Previous treatment lines (in chronological order)	Best response during all previous anti-PD-1 lines	Time from previous anti-PD-1 dose to first trial dose (days)	Percentage of viable tumor during the current trial		Clinical response in the current trial
					Pretreatment	Posttreatment	
Donor 1	1	D+T; Nivo; D+T reinduction; Ipi+Nivo	None	57	100	95	None
Donor 1	3	Pembro	None	66	100	30	Complete
Donor 1	5	Ipi+Nivo	Partial	119	100	<1	Partial
Donor 1	7	Pembro; D+T Nivo (adjuvant); Ipi; Carboplatin + Paclitaxel	Complete	204	80	30	Partial
Donor 1	9	Pembro; Ipi; Carboplatin + Paclitaxel	None	209	80	90	None
Donor 2	2	Pembro reinduction	Stable disease	114	N/A	N/A	None
Donor 2	4	Nivo (adjuvant)	None	112	85	90	None
Donor 2	6	Ipi; Pembro; D+T; Nivo; T-VEC + Nivo; TIL; D+T reinduction; Palbociclib; Carboplatin + Paclitaxel	Partial	322	100	85	None
Donor 2	8	Ipi+Nivo	Mixed	42	90	100	None
Donor 2	10	Ipi+Nivo	Stable disease	57	100	90	None

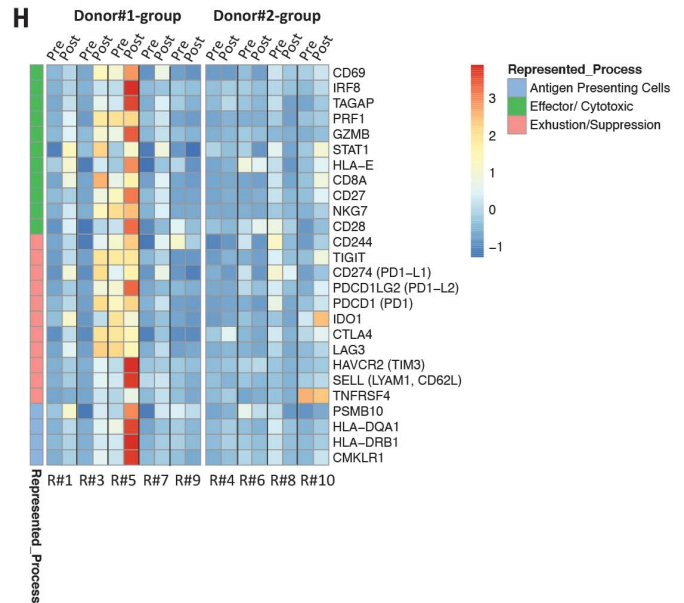
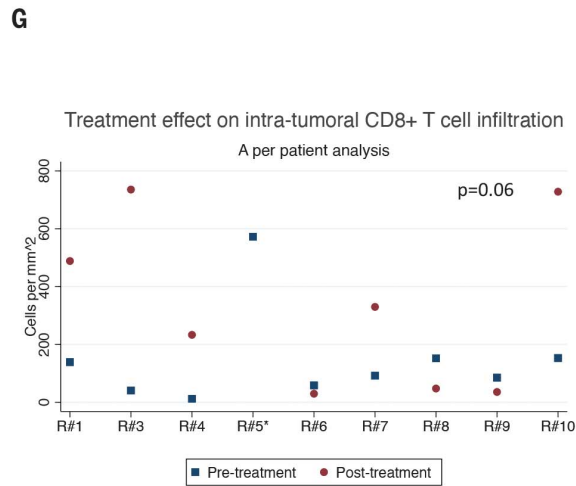
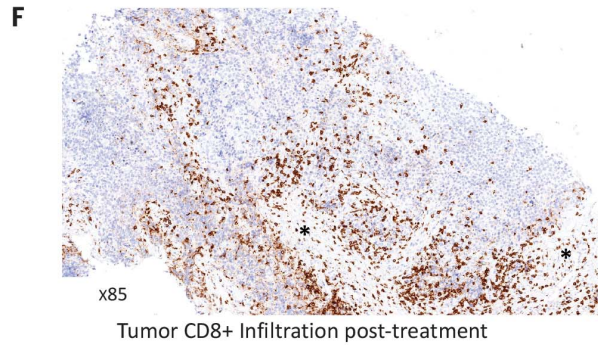
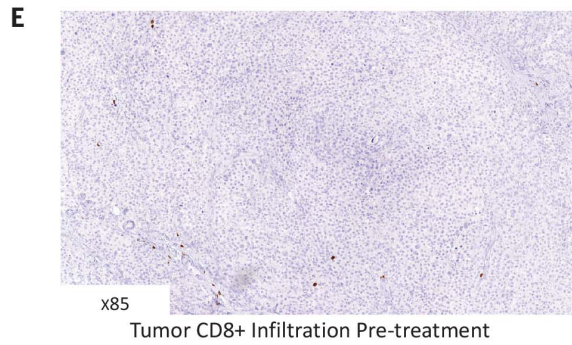
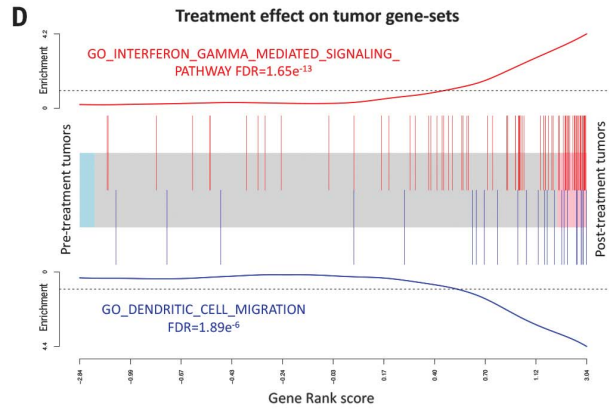
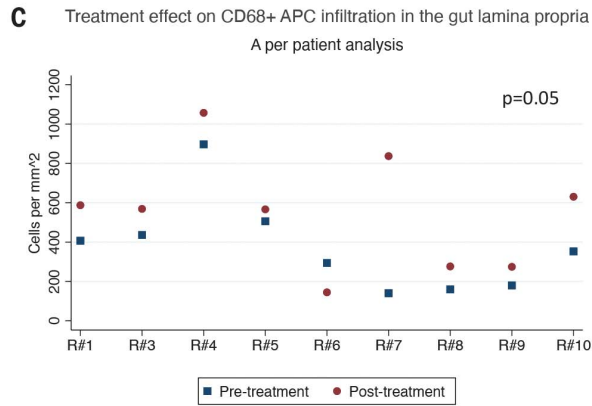
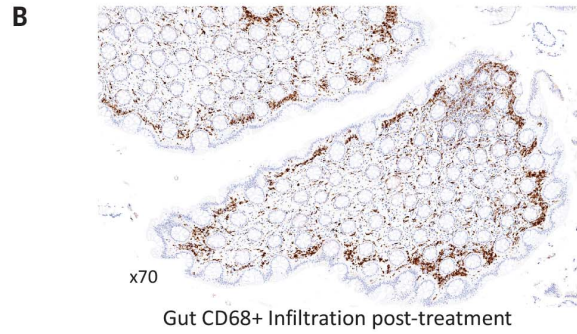
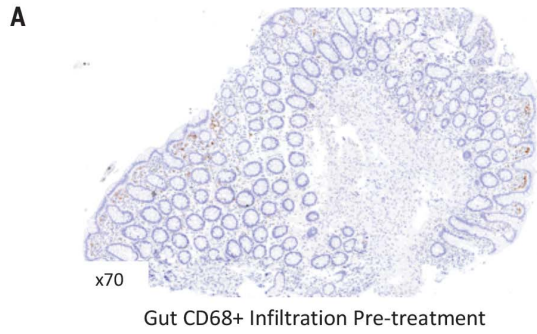


Fig. 3. The effect of FMT and reinduction of immunotherapy on immune activity in the gut and in the tumor microenvironment of metastatic melanoma recipient patients. (A) IHC staining of CD68, representing APCs, conducted on pretreatment sigmoid colon biopsies of recipient 7. (B) IHC staining of CD68⁺ cells conducted on the posttreatment (day 31) sigmoid colon biopsy of recipient 7, which demonstrates a clear increase in CD68⁺ cell infiltration in the gut lamina propria. This infiltration was especially prominent in the subepithelial area, which is physically closer to the gut. (C) An image analysis algorithm was used to quantify the number of CD68⁺ APCs within the gut lamina propria of each recipient patient. A posttreatment increment in CD68⁺ cell infiltration was demonstrated in most recipients ($P = 0.05$). (D) A barcode plot of gene set enrichment among tumor samples. Each bar represents a single gene out of the entire gene set. The plot demonstrates the up-regulation of APC- and T cell–related gene sets among posttreatment tumor samples. The full list of enriched gene sets is detailed in table S12. (E) IHC staining of CD8, representing cytotoxic T cells, conducted on pretreatment tumor metastasis (subcutaneous, left leg) of recipient 3. (F) IHC staining of CD8⁺ T cells conducted on posttreatment biopsy from another subcutaneous

metastasis in the left leg of recipient 3, demonstrating a clear increase in intratumoral CD8⁺ T cell infiltration and immune-induced tumor necrosis (marked by asterisks). (G) An image analysis algorithm was used to quantify the number of CD8⁺-stained T cells within viable tumor tissue for each remote tumor metastasis biopsy. Posttreatment tumor biopsies were preferably taken from the same metastasis used for the pretreatment biopsy or from another metastasis at the same organ. Five recipient patients had increased their intratumoral CD8⁺ T cell infiltration in posttreatment biopsies ($P = 0.06$). The asterisk indicates that recipient 5 achieved a near-pathological CR (<1% viable tumor), and hence their posttreatment CD8⁺ infiltration could not be accurately assessed. (H) Heatmap of tumor immune gene expression. The heatmap illustrates expression dynamics before and after treatment across three representative immune processes—antitumoral effector activity, suppression-exhaustion activity, and APCs activity-abundance. Only members of the donor 1 group demonstrated a posttreatment up-regulation of effector T cell response. Recipient 10 demonstrated a posttreatment up-regulation of the immune checkpoints IDO-1 and TIGIT without an effector response. Scale represents the z-score of gene counts.

microbiota compositions of the rest of the cohort. When the responders' posttreatment compositions were compared with the posttreatment compositions of the other two nonresponders from the donor 1 group (recipients 1 and 9), four taxa differed in a statistically significant manner (fig. S9A). The responders had a higher relative abundance of *Enterococcaceae*, *Enterococcus*, and *Streptococcus australis* and a lower relative abundance of *Veillonella atypica*. However, when the abundance of these specific taxa was assessed in the entire patient cohort (fig. S9B), there were some nonresponders and even pretreatment samples with similar dynamics. Hence, no clear association between those taxa and clinical response to therapy was established. Functional metabolic data were based on annotation of genes to the MetaCyc database (direct measurements of metabolite levels were not conducted). The functional metabolic data demonstrated that the donor 1 group up-regulated the lactose and galactose degradation I pathway [log-fold change (logFC) = 1; FDR = 0.015], whereas the donor 2 group up-regulated the formaldehyde assimilation II (logFC = 2.2; FDR = 3.93×10^{-6}), the formaldehyde oxidation I (logFC = 2.4; FDR = 0.001), and the creatinine degradation I (logFC = 1.4; FDR = 0.014) pathways. Metagenomics GO gene sets that significantly differed between the microbiota of the two donor groups are illustrated in Fig. 2C (table S8). Comparison between the posttreatment microbiota composition of the responding patients (recipients 3, 5, and 7) and the other two nonresponding patients (recipients 1 and 9) among the donor 1 group showed no significant functional or metabolic differences.

Gut sample analysis of all available FMT-recipient patients demonstrated a posttreatment up-regulation of gene sets that were related to the presentation of peptides by antigen-presenting cells (APCs) via major

histocompatibility complex (MHC) class I and interleukin-1–mediated signaling (FDR = 0.014 and 0.038, respectively; table S9). Analysis per donor group demonstrated that the donor 1–group recipients up-regulated additional gene sets related to APC activity, innate immunity, and interleukin-12 (table S10). By contrast, the donor 2–group recipients did not up-regulate any immune-related gene sets (table S11). Per-patient analysis demonstrated an increased lamina propria infiltration of CD68⁺ cells, representing APCs, from an overall pretreatment median of 353 to 569 cells/mm² posttreatment ($P = 0.05$; Fig. 3, A to C, and fig. S10). The CD68⁺ infiltration was concentrated in the subepithelial area, where the proximity to the gut lumen is the highest. All available recipients increased the posttreatment CD68⁺ infiltration except for recipient 6 (donor 2 group, nonresponder patient). Notably, gut sample analysis did not demonstrate a statistically significant increase in T cell infiltration in the gut lamina propria (fig. S11) or T cell–related gene set enrichment.

Tumor sample analysis of all available recipients demonstrated posttreatment up-regulation of multiple immune-related gene sets (Fig. 3D and table S12), such as interferon- γ –mediated signaling pathway (FDR = 1.65×10^{-13}), T cell activation (FDR = 3.27×10^{-12}), MHC class II protein complex (FDR = 9.31×10^{-13}), dendritic cell differentiation (FDR = 5.15×10^{-9}), and T helper 1–type immune response (FDR = 1.06×10^{-6}). Although these immune-related gene sets remained enriched in the donor 1 group–only analysis (table S13), no immune-related gene sets were statistically significantly enriched among tumor samples of the donor 2 group (table S14). Per-patient analysis demonstrated increased posttreatment intratumoral CD8⁺ T cell infiltration among five patients (recipients 1, 3, 4, 7, and 10) with an overall pretreatment median of 89 cells/mm²

versus 282 cells/mm² posttreatment ($P = 0.06$; Fig. 3, E to G, and fig. S12). Recipient 5 achieved a near-pathological CR, as posttreatment viable tumor tissue composed <1% of the entire biopsy, and recipients 3 and 7 achieved partial pathological response (Table 1). Assessment of commonly investigated genes related to intratumoral immune activity demonstrated that the posttreatment tumors of recipients 1, 3, 5, and 7 up-regulated effector-related genes with some reciprocal exhaustion responses (Fig. 3H). Recipient 10, however, up-regulated exhaustion-related genes without an effector response.

This study demonstrates that the combination of FMT from a CR donor and reinduction of anti-PD-1 therapy in refractory metastatic melanoma patients is safe, feasible, and potentially effective. FMT is considered a common treatment for recurrent *Clostridioides difficile* colitis, with a well-established safety profile (10), and its safety has been demonstrated even in immunocompromised patients (11). Nevertheless, the lack of FMT-related complications in this study among immunocompetent metastatic patients treated with repeated FMTs was reassuring. Notably, the combination of FMT and reinduction of anti-PD-1 therapy appeared safe and resulted in some objective clinical responses. Out of 10 anti-PD-1 refractory recipients, three demonstrated clinical responses, including one CR. A similar trial of FMT and anti-PD-1 reinduction in refractory melanoma patients has reported preliminary results of one objective partial response and one stable disease among the first three patients (12). Because the FMT-recipient patients were not treatment naïve, there is a possibility that these clinical outcomes are caused by delayed responses to previous anti-PD-1 treatments. However, this possibility is unlikely, as Ribas *et al.* have reported that delayed response rates in metastatic melanoma patients who continued

anti-PD-1 therapy beyond RECIST-confirmed disease progression were <8% (13). Similarly, Betof Warner *et al.* have reported that response rates of metastatic melanoma patients who were reintroduced with anti-PD-1 monotherapy were 5 out of 34 (<15%) (14). These results were possibly an overestimation because three of five responders in that study had an elapsed previous-to-reinduction dose time of at least 12 months (14). Such a prolonged time period might enable the reemergence of immunotherapy-susceptible tumor clones. In our study, the median previous-to-reinduction dose time was only 113 days among the entire cohort and 119 days among the three responders. Moreover, the inclusion criterion of our trial was disease progression on previous anti-PD-1 lines based on iRECIST. According to RECIST 1.1, partial responses or CRs may be deemed unconfirmed pending follow-up, but the classification of progressive disease is always considered final (15). However, immunotherapies might sometimes lead to pseudo-progression (8), as seen in recipients 3 and 5. iRECIST was designed to distinguish between unconfirmed and confirmed disease progression (7) (table S5). Hence, it is possible that the use of iRECIST in those previous publications would have resulted in even lower postfailure response rates.

This higher-than-expected clinical response rate can be explained by the correlative immunological data. Tumor-infiltrating dendritic cells (DCs) have a crucial role in trafficking T cells into tumors (16, 17). Multiple papers from mouse-model studies have demonstrated that microbiota modulation promoted the infiltration of DCs into remote tumors, which resulted in the activation of both T helper 1 cells via interleukin-12 (4, 18) and cytotoxic CD8⁺ T cells (19–21). The same findings were demonstrated in our human FMT trial. Because the donors' microbiotas were transplanted into the recipients' guts, it is plausible to assume that the immune activation cascade started in the gut. The donor 1-group recipients demonstrated increased posttreatment gut infiltration and activity of APCs. Geva-Zatorsky *et al.* have assessed the immune response to colonization of different commensal gut microbes and demonstrated that the local effect of microbes in the gut was mostly on the innate immunity cells (22), which could later migrate into the lymphatic system (23). Notably, some of the donor 2-group recipients also increased their posttreatment gut APC infiltration, although as a group, their RNA-seq findings were not statistically significant. Overall, the recipients who increased their posttreatment intratumoral CD8⁺ T cell infiltration also increased their APC gut infiltration. It is unlikely that the increment in CD8⁺ T cell infiltration was caused by the mere anti-PD-1 administration, because Chen *et al.* have used pre-

on-treatment tumor biopsies to demonstrate that nonresponding patients undergoing anti-PD-1 therapy did not increase their intratumoral CD8⁺ infiltration (24). However, microbiota-driven gut APC activation would not necessarily yield enhanced intratumoral CD8⁺ activity. Impaired antigen presentation machinery within the tumor cells themselves is a well-known anti-PD-1 resistance mechanism that usually results in lack of intratumoral CD8⁺ T cell infiltration (25). The tumor from recipient 9 demonstrated such an antigen presentation impairment (fig. S13). Moreover, even the presence of high intratumoral infiltration of CD8⁺ T cells sometimes fails to translate into a clinical response. Tumors with high CD8⁺ T cell infiltration can be refractory if the T cell infiltration is ineffective, for example as a result of CD8⁺ T cell exhaustion after exposure to additional immune checkpoints (26). Recipient 10 had overexpression of these molecules, such as IDO-1 (Fig. 3H). Recipient 1, who demonstrated increased intratumoral CD8⁺ T cell activity, had an initial regression in some metastases but eventually progressed as a result of an unknown cause. These tumor characteristics of different patients emphasize the wide context of clinical responses to immunotherapy and that beneficial microbiota composition is not the only factor in treatment response.

The microbiota composition of the two donors and the posttreatment recipients from both donor groups were characterized by high relative abundances of taxa that were previously associated with response to immunotherapy. Yet, the three responding recipients were solely part of the donor 1 group. The reason for this dissonance is unclear. However, this study was statistically powered to assess safety and was not designed to compare efficiency between donors. Lack of clinical responders among the donor 2 group does not necessarily implicate that clinical responses could not be observed in a larger cohort. Moreover, our inability to pinpoint specific response-inducer microbiota characteristics echoes the inconsistency among previous observational studies (6). As the characteristics of optimal microbiota compositions of donors and recipients remain elusive, the design and implementation of future microbiome modulation clinical trials must be carefully considered. Numerous considerations must be taken into account when contemplating strategies to modulate gut microbes, including diet (27). Studies in preclinical models incorporating microbiota into germ-free mice avatars may yield insight into both microbe and host factors. Nonetheless, in light of the decades-based safety profile of FMTs (10), promising results in preclinical models (2–4, 18, 19, 21), and findings that suggest treatment effectiveness in our current clinical trial, clinical institutions should not be deterred by the lack of sufficient mechanistic

knowledge to examine the clinical potential of FMTs in the setting of well-designed and supervised human trials. This is especially true for refractory patients, in whom the risk-to-benefit ratio of FMTs appears favorable.

One limitation of this clinical trial arises from the use of antibiotics as part of the pre-FMT preparation. Antibiotic preparation was adopted because it has enhanced the FMT ability to modulate microbiota composition in reported murine models (28). The vancomycin-neomycin protocol has been reported as an effective pre-FMT protocol in humans (29). Because all of our recipients underwent the exact same pre-FMT protocol, we believe that the use of antibiotics did not affect the observed immune and clinical outcomes. However, this possibility cannot be ruled out in the current study design.

FMT from CR donors and reinduction of anti-PD-1 therapy in refractory metastatic melanoma patients was demonstrated to be safe and feasible. In some patients, this treatment increased the intratumoral immune activity, which was translated into objective clinical responses. These findings support the concept of overcoming resistance to immunotherapy by modulating the gut microbiota.

REFERENCES AND NOTES

1. P. A. Ascierto *et al.*, *JAMA Oncol.* **5**, 187–194 (2019).
2. V. Gopalakrishnan *et al.*, *Science* **359**, 97–103 (2017).
3. V. Matson *et al.*, *Science* **359**, 104–108 (2018).
4. B. Routy *et al.*, *Science* **359**, 91–97 (2017).
5. Y. Belkaid, T. W. Hand, *Cell* **157**, 121–141 (2014).
6. V. Gopalakrishnan, B. A. Helmink, C. N. Spencer, A. Reuben, J. A. Wargo, *Cancer Cell* **33**, 570–580 (2018).
7. L. Seymour *et al.*, *Lancet Oncol.* **18**, e143–e152 (2017).
8. E. Borcoman *et al.*, *Ann. Oncol.* **30**, 385–396 (2019).
9. R. Verma *et al.*, *Sci. Immunol.* **3**, eaat6975 (2018).
10. U. Iqbal, H. Anwar, M. A. Karim, *Eur. J. Gastroenterol. Hepatol.* **30**, 730–734 (2018).
11. S. C. Lin, C. D. Alonso, A. C. Moss, *Transpl. Infect. Dis.* **20**, e12967 (2018).
12. G. Trinchieri, *Cancer Res.* **80**, IA28 (2020).
13. A. Ribas, J. M. Kirkwood, K. T. Flaherty, *Lancet Oncol.* **19**, e219 (2018).
14. A. Betof Warner *et al.*, *J. Clin. Oncol.* **38**, 1655–1663 (2020).
15. E. A. Eisenhauer *et al.*, *Eur. J. Cancer* **45**, 228–247 (2009).
16. S. Spranger, D. Dai, B. Horton, T. F. Gajewski, *Cancer Cell* **31**, 711–723.e4 (2017).
17. S. Spranger, T. F. Gajewski, *Oncol Immunology* **5**, e1086862 (2016).
18. M. Vétizou *et al.*, *Science* **350**, 1079–1084 (2015).
19. A. Sivan *et al.*, *Science* **350**, 1084–1089 (2015).
20. T. Tanoue *et al.*, *Nature* **565**, 600–605 (2019).
21. M. Uribe-Herranz *et al.*, *JCI Insight* **3**, e94952 (2018).
22. N. Geva-Zatorsky *et al.*, *Cell* **168**, 928–943.e11 (2017).
23. Z. Zhang *et al.*, *Immunity* **44**, 330–342 (2016).
24. P. L. Chen *et al.*, *Cancer Discov.* **6**, 827–837 (2016).
25. M. Sade-Feldman *et al.*, *Nat. Commun.* **8**, 1136 (2017).
26. J. A. Trujillo, R. F. Sweis, R. Bao, J. J. Luke, *Cancer Immunol. Res.* **6**, 990–1000 (2018).
27. J. L. McQuade, C. R. Daniel, B. A. Helmink, J. A. Wargo, *Lancet Oncol.* **20**, e77–e91 (2019).
28. S. K. Ji *et al.*, *Front. Microbiol.* **8**, 1208 (2017).
29. J. Ni *et al.*, *Sci. Transl. Med.* **9**, eaah6888 (2017).

ACKNOWLEDGMENTS

This study was conducted in honor of the memory of Allen S. Berg. We wish to thank the Lemelbaum family for its support, O. Mazuz for assisting in trial coordination, M. Davies for his thoughtful insights, A. Lipsky for assisting in the statistical design of the clinical trial, M. Stern for performing most of the tumor biopsies, N. Nissan for assisting in acquiring

radiological data, Y. Glick for assisting with the RNA-seq analysis, G. Smollan for assisting in the donor screening process, M. Shaharabany and A. Nachmani for their technical support in the use of the Aperio scanner, N. Keidar and N. Orbach-Zingboim for designing the suggested diet, D. Binyamin for assisting in the 16S rRNA gene sequencing analysis, and the patients and their families. **Funding:** This trial was funded only by the Ella Lemelbaum Institute for Immuno-Oncology internal funds. E.N.B. was supported by the Allen Berg Fund for Excellence in Immuno-Oncology Research, Young Researcher Scholarship. G.M. was supported by the Henry and Susan Samueli Foundation Grant for Integrative Immuno-Oncology. **Author contributions:** Conceptualization: B.B., G.M., and E.N.B.; Formal analysis and software: E.N.B., N.B., K.A., M.A., M.A.W.K., and N.J.A.; Funding acquisition: G.M. and J.S.; Investigation: E.N.B., R.O., S.B.-S., O.Z., J.M., D.D.-N., D.R., K.A., L.A., C.A., G.B.-B., L.K., T.B.-N., S.R., A.L., Y.S.-S., Y.E., H.H., N.A., and R.S.-F.; Methodology: E.N.B., B.B., I.Y., R.O., L.K., T.B.-N., R.M., O.K., L.K., A.L., and I.B.; Project administration: E.N.B. and R.O.; Resources: G.M., O.K., I.Y., I.B., and J.S.; Supervision: G.M., B.B., J.S., I.B., I.Y., O.K., and J.A.W.; Visualization: E.N.B., S.R., N.J.A., K.A., N.B., and M.A.W.K.; Writing – original draft: E.N.B.; Writing – review and editing: E.N.B., B.B., I.Y., G.M., M.A., N.J.A., R.M., J.S., and

J.A.W. **Competing interests:** I.Y. is a medical adviser for Mybiotix Ltd. G.B.-B. received honoraria and travel support from MSD, Roche, BMS, Novartis, and Medison. Y.S.-S. received honoraria from MSD, Roche, BMS, and Novartis. N.A. received honoraria from MSD, Roche, BMS, Novartis, and Medison. R.S.-F. received honoraria from MSD and BMS. J.S. received honoraria from MSD, Roche, BMS, and Novartis; serves on the advisory boards of MSD, BMS, and Novartis; owns shares of 4c BioMed; and is partially employed by 4cBiomed. J.A.W. is an inventor on a U.S. patent application (PCT/US17/53,717) submitted by the University of Texas MD Anderson Cancer Center that covers methods to enhance immune checkpoint blockade responses by modulating the microbiome; reports compensation for speaker's bureau and honoraria from Imedex, Dava Oncology, Omniprex, Illumina, Gilead, PeerView, Physician Education Resource, MedImmune, Exelixis, and Bristol-Myers Squibb; serves as a consultant and/or advisory board member for Roche/Genentech, Novartis, AstraZeneca, GlaxoSmithKline, Bristol-Myers Squibb, Merck, Biothera Pharmaceuticals, and Microbiome DX; and receives research support from GlaxoSmithKline, Roche/Genentech, Bristol-Myers Squibb, and Novartis. G.M. received honoraria from MSD, Roche, BMS, and Novartis; received research grants from Novartis and BMS (not related to this study); serves on the advisory board of MSD, NucleAI, and Biond

Biologics; holds IP and shares of Kitov and 4cBiomed; and is partially employed by 4cBiomed. The rest of the authors declare no competing interests. **Data and materials availability:** Microbiome 16S rRNA and metagenomics sequencing data have been deposited in the National Center for Biotechnology Information (NCBI) Sequence Read Archive (SRA) under BioProject ID PRJNA678737. The human gut and tumor RNA-seq data have been deposited at the NCBI Gene Expression Omnibus (GEO) under BioProject ID GSE162436.

SUPPLEMENTARY MATERIALS

science.sciencemag.org/content/371/6529/602/suppl/DC1
Materials and Methods
Supplementary Text
Figs. S1 to S13
Tables S1 to S15
References (30–64)
MDAR Reproducibility Checklist

[View/request a protocol for this paper from Bio-protocol.](#)

6 March 2020; accepted 1 December 2020
Published online 10 December 2020
10.1126/science.abb5920

Fecal microbiota transplant promotes response in immunotherapy-refractory melanoma patients

Erez N. Baruch, Ilan Youngster, Guy Ben-Betzalel, Rona Ortenberg, Adi Lahat, Lior Katz, Katerina Adler, Daniela Dick-Necula, Stephen Raskin, Naamah Bloch, Daniil Rotin, Liat Anafi, Camila Avivi, Jenny Melnichenko, Yael Steinberg-Silman, Ronac Mamtani, Hagit Harati, Nethanel Asher, Ronnie Shapira-Frommer, Tal Brosh-Nissimov, Yael Eshet, Shira Ben-Simon, Oren Ziv, Md Abdul Wadud Khan, Moran Amit, Nadim J. Ajami, Iris Barshack, Jacob Schachter, Jennifer A. Wargo, Omry Koren, Gal Markel and Ben Boursi

Science **371** (6529), 602-609.
DOI: 10.1126/science.abb5920originally published online December 10, 2020

New fecal microbiota for cancer patients

The composition of the gut microbiome influences the response of cancer patients to immunotherapies. Baruch *et al.* and Davar *et al.* report first-in-human clinical trials to test whether fecal microbiota transplantation (FMT) can affect how metastatic melanoma patients respond to anti-PD-1 immunotherapy (see the Perspective by Woelk and Snyder). Both studies observed evidence of clinical benefit in a subset of treated patients. This included increased abundance of taxa previously shown to be associated with response to anti-PD-1, increased CD8⁺ T cell activation, and decreased frequency of interleukin-8-expressing myeloid cells, which are involved in immunosuppression. These studies provide proof-of-concept evidence for the ability of FMT to affect immunotherapy response in cancer patients.

Science, this issue p. 602, p. 595; see also p. 573

ARTICLE TOOLS

<http://science.sciencemag.org/content/371/6529/602>

SUPPLEMENTARY MATERIALS

<http://science.sciencemag.org/content/suppl/2020/12/09/science.abb5920.DC1>

RELATED CONTENT

<http://stm.sciencemag.org/content/scitransmed/11/522/eaax2693.full>
<http://stm.sciencemag.org/content/scitransmed/12/526/eaax7992.full>
<http://stm.sciencemag.org/content/scitransmed/12/530/eaax0876.full>
<http://stm.sciencemag.org/content/scitransmed/12/535/eaaz8235.full>
<http://science.sciencemag.org/content/sci/371/6529/573.full>

REFERENCES

This article cites 62 articles, 18 of which you can access for free
<http://science.sciencemag.org/content/371/6529/602#BIBL>

PERMISSIONS

<http://www.sciencemag.org/help/reprints-and-permissions>

Use of this article is subject to the [Terms of Service](#)

Science (print ISSN 0036-8075; online ISSN 1095-9203) is published by the American Association for the Advancement of Science, 1200 New York Avenue NW, Washington, DC 20005. The title *Science* is a registered trademark of AAAS.

Copyright © 2021 The Authors, some rights reserved; exclusive licensee American Association for the Advancement of Science. No claim to original U.S. Government Works